Dalton Transactions

ROYAL SOCIETY OF CHEMISTRY

COMMUNICATION

View Article Online
View Journal | View Issue

Cite this: *Dalton Trans.*, 2025, **54**, 1365

Received 19th November 2024,
Accepted 12th December 2024

DOI: 10.1039/d4dt03243h

rsc.li/dalton

An electrospray-active N-heterocyclic carbene ligand for real-time analysis of organometallic reactions†

Charles Killeen, *[a] Allen G. Oliver [b] and J. Scott McIndoe *[a]

A charge-tagged N-heterocyclic carbene (NHC) has been synthesized and its utility in allowing the dynamic behaviour of metal complexes to be monitored in real time using electrospray ionization mass spectrometry demonstrated. This compound was used to prepare different metal-NHC complexes, and the kinetic behaviour of complex formation and ligand exchange was monitored in real time through the use of pressurized sample infusion electrospray mass spectrometry (PSI-ESI-MS).

The solubilizing, strong σ-donating, and steric shielding properties of N-heterocyclic carbene (NHC) ligands make them excellent scaffolds for building discrete molecular homogenous catalysts, and their utility has been continuously demonstrated since their introduction in the mid-1990s. NHCs represent a particularly stable type of compound that contains a formally divalent carbon atom. Their existence was proposed in 1962 by Wanzlick, who showed a minor equilibrium population of free carbene is formed from dissociation of tetraaminoethylene dimers.[1] The first example of an isolable NHC was synthesized by Arduengo in 1991, who exploited the steric bulk of adamantyl groups to prevent dimerization. Though the direct synthesis of metal-NHC complexes from protonated imidazolium salts was first shown in the 1968 synthesis of bis-(1,3-diphenylimidazolium)mercury(II) perchlorate,[2] the catalytic activity of metal-NHC complexes was first realized in the 1995 application of bis-NHC palladium complexes to the Heck alkenylation of chloroarenes.[3] Shortly following the reported olefin metathesis activity of bis-NHC ruthenium(II) alkylidene complexes,[4] the immense synthetic utility of the mono-NHC ruthenium alkylidene complexes bearing one phosphine ligand was discovered.[5–7] These Grubbs second generation catalysts benefitted from improved initiation rates and air- and moisture-stability,[8] and many compounds of this type still find widespread use in olefin metathesis chemistry today. The utility of NHCs as ligands supporting discrete homogenous palladium catalysts has made them a major player in modern catalyst development.[9,10]

The function of NHC ligands in homogenous catalysis is multifaceted. The typically bulky aromatic substituents on the nitrogen atoms of the heterocycle confer good organic solubility through non-covalent interactions, and their "umbrella" shape effectively shields the active metal centre, allowing formation of low coordinate complexes while preventing unwanted side reactions such as dimerization. NHCs have a similarly wide range of steric bulk available as phosphine ligands, and their stronger σ-donation ability[11] renders them better spectator ligands due to their stronger binding to metal centres (Fig. 1).

Electrospray ionization mass spectrometry (ESI-MS) is an invaluable tool for the mechanistic and kinetic analysis of organometallic reactions and catalysis.[12–16] With the development of pressurized sample infusion ESI-MS (PSI-ESI-MS), real-time mass spectrometric monitoring of air- and moisture-sensitive reactions has become routine.[17] This technique is greatly bol-

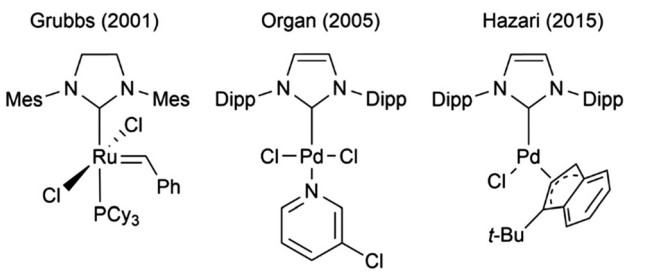

Fig. 1 Examples of homogenous catalysts that use N-heterocyclic carbene ligands. (Mes = 2,4,6-trimethylphenyl, Dipp = 2,6-diisopropylphenyl).

[a]*Department of Chemistry, University of Victoria, P.O. Box 3065, Victoria, BC V8W 3 V6, Canada. E-mail: ckilleen@uvic.ca, mcindoe@uvic.ca*
[b]*Department of Chemistry and Biochemistry, University of Notre Dame, Notre Dame, Indiana 46556, USA*

†Electronic supplementary information (ESI) available: Synthetic and experimental procedures, NMR and mass spectral data. CCDC 2391546. For ESI and crystallographic data in CIF or other electronic format see DOI: https://doi.org/10.1039/d4dt03243h

Fig. 2 Structural elements of the imidazolinium NHC-precursor, highlighting the three conceptual building block elements of the heterocyclic ring.

stered by the synthetic strategy of "charge-tagging" ligands and/or substrates, that being the addition of cationic or anionic groups to molecules of interest.[18] Analytes having charged groups already present obviates the need for in-source ionization during the ESI process, facilitating the use of softer ESI conditions during analysis. The gentler conditions minimize in-source fragmentation, which can preserve weakly bound structural elements. The high dynamic range of ESI-MS allows species which are many orders of magnitude less abundant than reactants and products to be readily detected, and the charge-tagging of catalysts strategy further facilitates this end.

Previous ESI-MS studies of charged NHCs have focused mainly on their reactivity towards carbon dioxide in the gas phase,[19,20] though their use in investigating other organic transformations has been shown in the monitoring of Stetter-type reactions between a thiazolium carbene and benzaldehyde.[21,22] Existing charged NHC studies are typically based on alkylated imidazole, thiazole, or triazole carbenes, which are reminiscent of common ionic liquids. The charged moieties in these systems are typically alkyl-tethered carboxylates[23] or sulfonates[21,22] in the anionic case, and an additional cationic heterocycle in the positive case, where one of the two heterocycles forms the divalent carbon species.[24]

An acceptable charge-tagged moiety must fulfill a few requirements to be compatible both with the chemistry in question and the PSI-ESI-MS technique. First and foremost, charge-tagged ligands and substrates must be chemically inert and confer solubility in the same solvent in which the analogous non-ionic chemistry would be performed. Additionally, the inclusion of structural elements which promote high ESI response greatly favours detecting species in low abundance, such as intermediates, by-products, and off-cycle species.[25] There are numerous examples of charged NHC ligands for aqueous catalysis in literature,[26–29] with some finding use in commercialized catalysts such as AquaMet, which is used for aqueous olefin metathesis.[30] However, the set of properties which make a charged NHC amenable to aqueous chemistry are typically antithetical to the charge-tagging strategy in ESI-MS reaction monitoring, which seeks to keep reaction conditions as close to the non-ionic counterpart as possible. Such substituents, exemplified by the cationic trimethylammonium ion and the anionic sulfonate anion, have high charge localization and minimal steric bulk. As a result, these ions are highly coordinating, minimizing the ability of their salts to

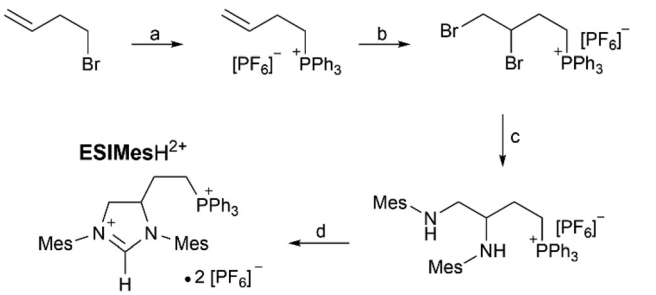

Scheme 1 Synthetic route to the described charged NHC proligand **ESIMes**H^{2+}. (a) PPh_3 (1.2 eq.), toluene, reflux, 24 h, then $NaPF_6$, MeOH/H_2O. (b) Br_2, 1,2-dichloroethane, rt, 0.5 h. (c) 2,4,6-Trimethylaniline (5 eq.), neat, 125 °C, 24 h. (d) Triethyl orthoformate (10 eq.), NH_4PF_6 (1 eq.), HCOOH (cat.), 3.5 h.

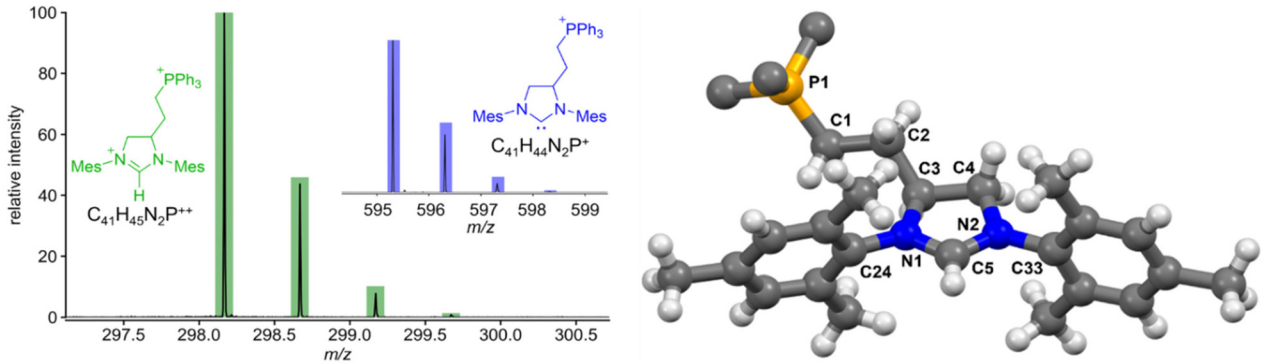

Fig. 3 (left) ESI-MS spectra of [**ESIMes**H^{2+}] (green) with its deprotonated form with [**ESIMes**]$^+$ (blue) inlayed, illustrating the doubly charged proligand and singly charged divalent carbene species formed during ESI. (right) Refined X-ray structure of **ESIMes**H^{2+}, with only the *ipso* phenyl carbon atoms on phosphorus shown for clarity (see ESI† for full structure). Key bond lengths and angles: P1–C1: 1.802(9) Å, C1–C2 1.533(11) Å, C2–C3 1.551(10) Å, C3–C4 1.533(12) Å, C3–N1 1.498(9) Å, C4–N2 1.485(9) Å, C5–N1 1.320(9) Å, C5–N2 1.305(10) Å, N1–C24 1.440(10) Å, N2–C33 1.443(10) Å, C1–C2–C3 110.9(6)°, C2–C3–C4 113.6(6)°, N1–C3–C4 102.1(5)°, N2–C4–C3 103.0(6)°, C4–N2–C5 110.2(6)°, C3–N1–C5 109.6(6)°, C3–N1–C24 124.0(6)°, C4–N2–C33 123.4(6)°, C5–N1–C24 126.3(6)°, C5–N2–C33 126.4(6)°, N1–C5–N2 113.8(6)°.

dissolve in moderately polar organic solvents typical of traditional NHC catalysis, though some use of anionic tethered NHC-sulfonates in polar organic solvents has been shown.[31] A particularly useful and ESI-responsive charge-tag moiety is the triphenylphosphonium cation, which has been exploited in a multitude of ESI-MS studies.[25,32–35] The exceptionally high response arises from a few factors, including structural rigidity and the mix of steric shielding and charge delocalization[36] minimizing ion–dipole interactions with solvent molecules that inhibit analytes from entering the gas phase during ESI-MS.[25] The alkyltriphenylphosphonium unit is typically chemically inert other than toward very strong bases and some basic organometallics,[37] and was chosen as the best charge-tagged structural element for an ESI-active NHC ligand.

Before engaging in a synthetic campaign, the most logical location for the charge-tagged moiety was assessed. The carbon backbone (see Fig. 2) of the pre-carbenic structure was considered a better choice than the nitrogen atom substituents for a few reasons. As the synthesis of NHC proligands typically involves two aniline nucleophiles, structural modification of that element would either give a doubly charge-tagged NHC ligand or involve a more challenging stepwise synthesis with two different anilines. Additionally, the large steric bulk of the triphenylphosphonium group would increase the already large steric bulk of these flanking units should it be located there. For these reasons, the best location for the charged phosphonium group was determined to be on the carbon backbone of the proligand. An ethylene linker was chosen to move the steric bulk of the triphenylphosphonium group away from the active site, while minimizing the "greasiness" of excessive alkyl chain length (Fig. 3).

Triphenylphosphine is a competent nucleophile for the S_N2 reaction with 4-bromobut-1-ene, forming (but-1-enyl)triphenylphosphonium bromide, which is subsequently subjected to anion exchange forming the hexafluorophosphate salt (Scheme 1a). Bromination of the alkene gives the dibromoalkane (Scheme 1b), which is an appropriate electrophile for subsequent nucleophilic attack by 2,4,6-trimethylaniline (Scheme 1c). A subsequent acid-catalyzed cyclization was carried out with triethyl orthoformate as the C2 carbon source (Scheme 1d). The successful synthesis of the desired product was confirmed by NMR spectroscopy, ESI-MS, and single crystal X-ray diffraction. The product imidazolinium has a characteristic sharp singlet in the ^{1}H NMR spectrum at 8.16 ppm (CD_3CN) which arises from the C2 carbon C–H bond. The ESI-MS(+) spectrum of the product shows a significant peak with a major isotopomer at *m*/*z* 298.1669 (Δ = 4.7 ppm), with the 0.5 Da gap between peaks indicative of the doubly cationic species [**ESIMesH**]$^{2+}$. The other two major signals at *m*/*z* 595 and 741 indicate free [**ESIMes**]$^+$ and [**ESIMesH** + PF_6]$^+$ respectively, with the abundance of free [**ESIMes**]$^+$ being more prominent in polar coordinating solvents.

The first metal complex synthesized as a proof of concept with the [**ESIMes**]$^+$ ligand was the silver bis-NHC complex, which forms as a triply-charged cation (Fig. 4). The double ligation is likely due to the weak coordinative ability of the hexafluorophosphate anion, which allows the addition of a second carbene ligand at the metal centre.

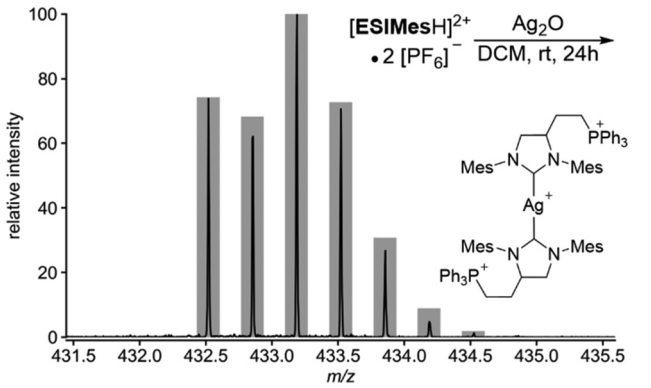

Fig. 4 Synthetic pathway and ESI(+) spectrum of a silver bis-(**ESIMes**) complex, with the theoretical isotope pattern overlay for [Ag(**ESIMes**)$_2$]$^{3+}$.

The attempted synthesis of a Cu(I)**ESIMes** complex with CuBr and K_2CO_3 in dichloromethane gave instead the double salt ([**ESIMesH**]$^{2+}$[$CuBr_2$]$^-$[PF_6]$^-$) upon workup and isolation. The dehydrobromination of this compound with the organic-soluble base diazabicycloundecene (DBU) in dichloromethane formed the Cu(I)**ESIMes** complex rapidly. As a result, we were able to monitor this process in real time *via* PSI-ESI-MS. There is an interesting kinetic feature in this system, where there is an apparent delay between the signal of the pre-complex ion pair disappearing and the complex signal appearing. We ascribe this behavior to a formally neutral (and hence ESI-invisible) zwitterionic intermediate forming, indicating that the dehydrobromination is a stepwise process in this case (Fig. 5).

Finally, a more air-sensitive and catalytically interesting group 9 metal **ESIMes** complex was investigated. For this experiment we endeavored to follow *in situ* the formation of an iridium NHC complex from [**ESIMesH**]$^{2+}$ dihexafluoropho-

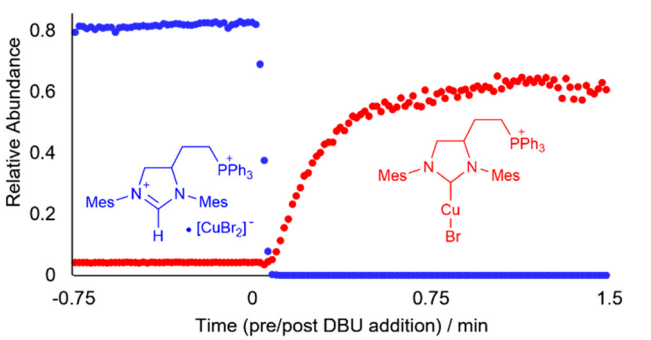

Fig. 5 PSI-ESI-MS kinetic data of copper **ESIMes** complex formation dynamics, showing the dehydrobromination of the ion pair [**ESIMesH**]$^{2+}$[$CuBr_2$]$^-$ (blue) to the Cu(I)**ESIMes** complex (red). See ESI, Fig. S15 and S16† for isotope pattern overlay.

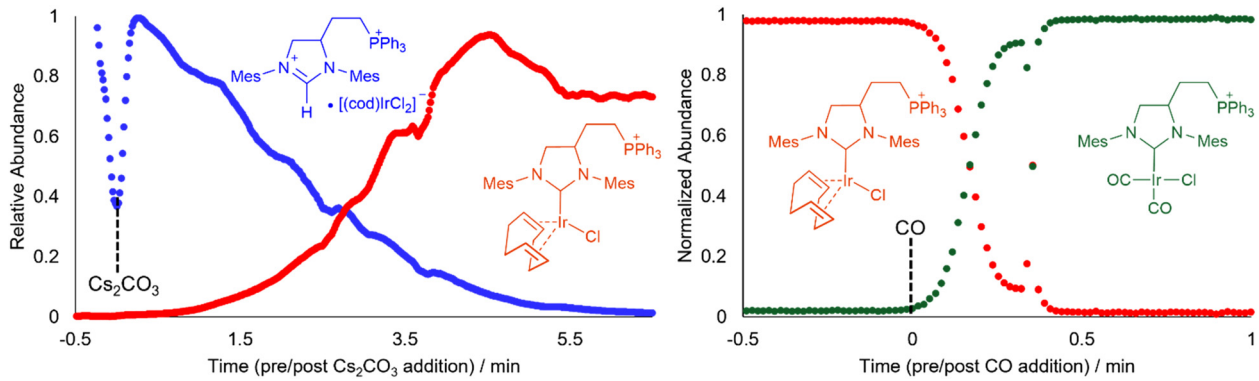

Fig. 6 (left) Iridium **ESIMes** complex formation dynamics, showing a in initial ion pair (blue) which is dehydrochlorinated into the resulting iridium **ESIMes** complex. A 10 μM solution of [**ESIMes**H]$^{2+}$ dihexafluorophosphate and (Ir(cod)Cl)$_2$ in dichloromethane was heated to 40 °C and stirred while being infused into the ESI source until the signal of the ion paired species stabilized, at which time 5 mg Cs_2CO_3 was quickly added during a break in system pressure. (right) Iridium **ESIMes** complex ligand displacement kinetics, showing the displacement of the cyclooctadiene ligand by two carbonyl ligands.

sphate and (Ir(cod)Cl)$_2$, and then a subsequent substitution of the cyclooctadiene ligand at the metal centre using carbon monoxide. Like the copper **ESIMes** system, the base was added last to this system, in this case Cs_2CO_3, which accounts for the signal drop seen at t = 0 min in the PSI-ESI-MS spectrum (Fig. 6) as pressurized sample infusion is temporarily interrupted. After complex formation, the cyclooctadiene ligand is rapidly displaced by injecting a small volume (5 mL) of carbon monoxide into the headspace of the vessel, forming the iridium dicarbonyl compound, as shown in Fig. 6 (for isotope pattern overlays see ESI, Fig. S17 and S18†). After formation, this complex was subjected to MS/MS, where it fragmented predictably with loss of one and two carbonyl ligands (Fig. S19†). The use of this charge-tagged NHC ligand has shown to be valuable in identifying and monitoring the kinetic and dynamic behaviour of metal-NHC complex formation and ligand substitution in real time. Continuing work using this ligand in tandem with the PSI-ESI-MS technique for monitoring catalytic reactions, competitive substrate binding, and catalyst degradation processes will help to further the understanding of the chemistry of such metal-NHC complexes and the reaction dynamics of the chemistry that they participate in.

Data availability

All experimental procedural data, synthetic procedural data, NMR and mass spectrometric data, and a copy of the crystallographic data are found in the ESI.† Additionally, the .cif (CCDC 2391546†) file for the X-ray structure of this complex has been uploaded to the CCDC.

Conflicts of interest

There are no conflicts to declare.

Acknowledgements

JSM thanks NSERC for operational (Discovery Grant) and infrastructural (Research Tools and Instruments Grant) support, and the University of Victoria for infrastructure support. Funding for the Bruker Venture was supported by NSF MRI Award CHE-2214606.

References

1 H. W. Wanzlick, *Angew. Chem., Int. Ed. Engl.*, 1962, **1**, 75–80.
2 H.-W. Wanzlick and H.-J. Schönherr, *Angew. Chem., Int. Ed. Engl.*, 1968, **7**, 141–142.
3 W. A. Herrmann, M. Elison, J. Fischer, C. Köcher and G. R. J. Artus, *Angew. Chem., Int. Ed. Engl.*, 1995, **34**, 2371–2374.
4 T. Weskamp, W. C. Schattenmann, M. Spiegler and W. A. Herrmann, *Angew. Chem., Int. Ed.*, 1998, **37**, 2490–2493.
5 L. Ackermann, A. Fürstner, T. Weskamp, F. J. Kohl and W. A. Herrmann, *Tetrahedron Lett.*, 1999, **40**, 4787–4790.
6 J. Huang, E. D. Stevens, S. P. Nolan and J. L. Petersen, *J. Am. Chem. Soc.*, 1999, **121**, 2674–2678.
7 M. Scholl, S. Ding, C. W. Lee and R. H. Grubbs, *Org. Lett.*, 1999, **1**, 953–956.
8 M. Scholl, T. M. Trnka, J. P. Morgan and R. H. Grubbs, *Tetrahedron Lett.*, 1999, **40**, 2247–2250.
9 C. J. O'Brien, E. A. B. Kantchev, C. Valente, N. Hadei, G. A. Chass, A. Lough, A. C. Hopkinson and M. G. Organ, *Chem. – Eur. J.*, 2006, **12**, 4743–4748.
10 P. R. Melvin, A. Nova, D. Balcells, W. Dai, N. Hazari, D. P. Hruszkewycz, H. P. Shah and M. T. Tudge, *ACS Catal.*, 2015, **5**, 3680–3688.
11 G. C. Fortman and S. P. Nolan, *Chem. Soc. Rev.*, 2011, **40**, 5151.
12 P. Chen, *Angew. Chem., Int. Ed.*, 2003, **42**, 2832–2847.
13 J. S. McIndoe and K. L. Vikse, *J. Mass Spectrom.*, 2019, **54**, 466–479.

14 B. Zimmer, T. Auth and K. Koszinowski, *Chem. – Eur. J.*, 2023, **29**, e202300725.
15 E. A. Denisova, A. Y. Kostyukovich, A. N. Fakhrutdinov, V. A. Korabelnikova, A. S. Galushko and V. P. Ananikov, *ACS Catal.*, 2022, **12**, 6980–6996.
16 A. Bütikofer, V. Kesselring and P. Chen, *Organometallics*, 2024, **43**, 934–946.
17 G. T. Thomas, S. Donnecke, I. C. Chagunda and J. S. McIndoe, *Chem. Methods*, 2022, **2**, e202100068.
18 D. M. Chisholm and J. S. McIndoe, *Dalton Trans.*, 2008, 3933.
19 P. M. Lalli, T. S. Rodrigues, A. M. Arouca, M. N. Eberlin and B. A. D. Neto, *RSC Adv.*, 2012, **2**, 3201.
20 C. Salvitti, I. Chiarotto, F. Pepi and A. Troiani, *ChemPlusChem*, 2021, **86**, 209–223.
21 H. Zeng, K. Wang, Y. Tian, Y. Niu, L. Greene, Z. Hu and J. K. Lee, *Int. J. Mass Spectrom.*, 2014, **369**, 92–97.
22 Y. Tian and J. K. Lee, *J. Org. Chem.*, 2015, **80**, 6831–6838.
23 C. Salvitti, F. Pepi, M. Managò, M. Bortolami, C. Michenzi, I. Chiarotto, A. Troiani and G. De Petris, *Rapid Commun. Mass Spectrom.*, 2022, **36**, e9338.
24 M. Paul, E. Detmar, M. Schlangen, M. Breugst, J. Neudörfl, H. Schwarz, A. Berkessel and M. Schäfer, *Chem. – Eur. J.*, 2019, **25**, 2511–2518.
25 I. Omari, P. Randhawa, J. Randhawa, J. Yu and J. S. McIndoe, *J. Am. Soc. Mass Spectrom.*, 2019, **30**, 1750–1757.
26 A. Ferry, K. Schaepe, P. Tegeder, C. Richter, K. M. Chepiga, B. J. Ravoo and F. Glorius, *ACS Catal.*, 2015, **5**, 5414–5420.
27 L. Schaper, S. J. Hock, W. A. Herrmann and F. E. Kühn, *Angew. Chem., Int. Ed.*, 2013, **52**, 270–289.
28 J. M. Asensio, R. Andrés, P. Gómez-Sal and E. De Jesús, *Organometallics*, 2017, **36**, 4191–4201.
29 J. M. Asensio, S. Tricard, Y. Coppel, R. Andrés, B. Chaudret and E. de Jesús, *Chem. – Eur. J.*, 2017, **23**, 13435–13444.
30 K. Skowerski, G. Szczepaniak, C. Wierzbicka, Ł. Gułajski, M. Bieniek and K. Grela, *Catal. Sci. Technol.*, 2012, **2**, 2424.
31 Y. Yuan, C. Chen, C. Zeng, B. Mousavi, S. Chaemchuen and F. Verpoort, *ChemCatChem*, 2017, **9**, 882–887.
32 L. P. E. Yunker, R. L. Stoddard and J. S. McIndoe, *J. Mass Spectrom.*, 2014, **49**, 1–8.
33 C. Adlhart and P. Chen, *HCA*, 2000, **83**, 2192–2196.
34 H. Woo, E. P. Go, L. Hoang, S. A. Trauger, B. Bowen, G. Siuzdak and T. R. Northen, *Rapid Commun. Mass Spectrom.*, 2009, **23**, 1849–1855.
35 A. Lizzul-Jurse, L. Bailly, M. Hubert-Roux, C. Afonso, P.-Y. Renard and C. Sabot, *Org. Biomol. Chem.*, 2016, **14**, 7777–7791.
36 T. A. Trendeleva, E. I. Sukhanova, A. G. Rogov, R. A. Zvyagilskaya, I. I. Seveina, T. M. Ilyasova, D. A. Cherepanov and V. P. Skulachev, *Mitochondrion*, 2013, **13**, 500–506.
37 A. Federov, M. Moret and P. Chen, *J. Am. Chem. Soc.*, 2008, **130**, 8880–8881.